

Figure S1. Description of salivary gland degradation defect phenotype. Related to Figure 1

A histological section (left) of an animal 24h after puparium formation with a salivary gland degradation defect (*fkh-GAL4/w; UAS-CG8177^{IR}/+; +*). The persistent salivary gland tissue has been highlighted by removal of the surrounding tissues (right).

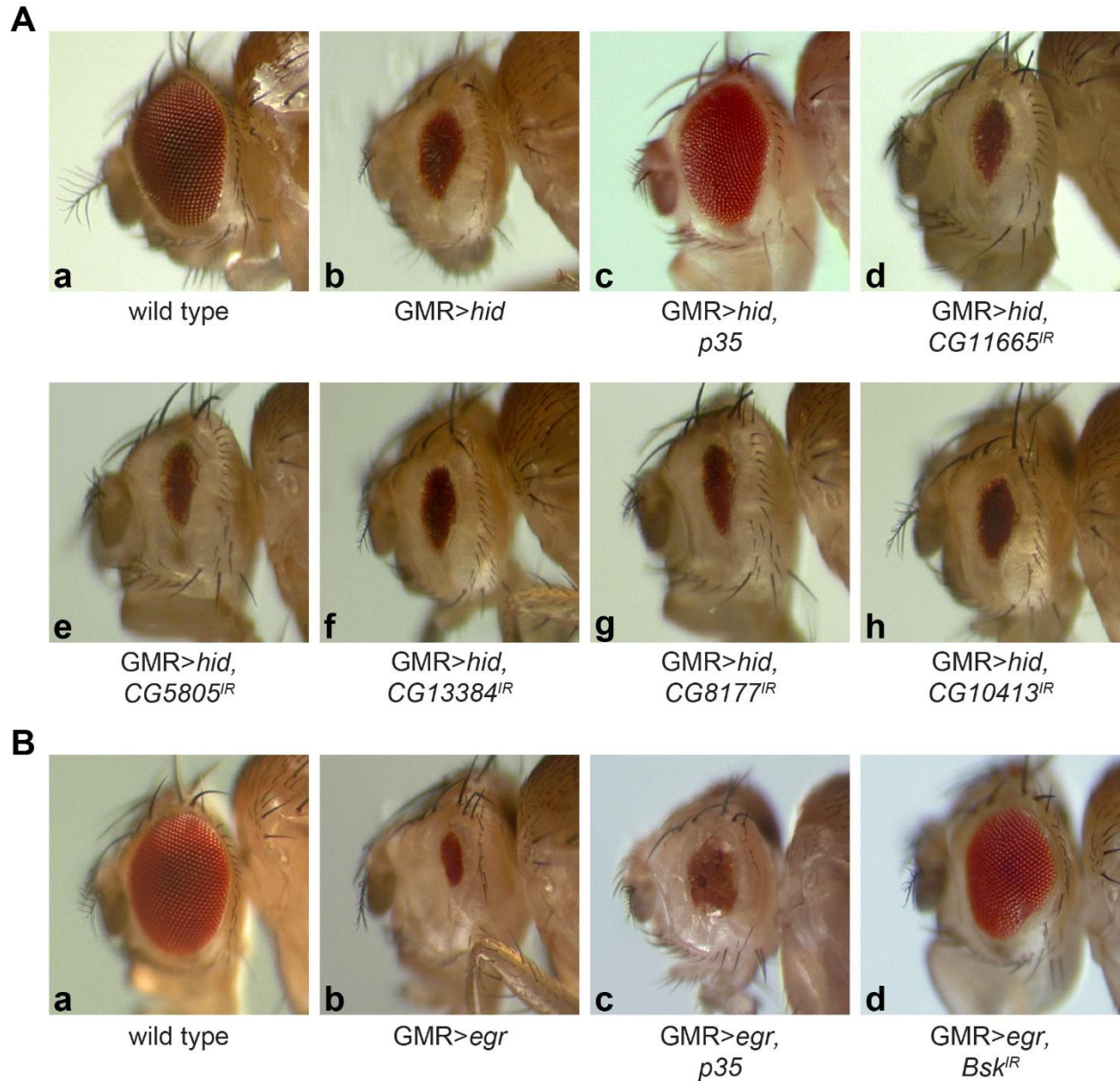


Figure S2. The identified *SLC* genes do not suppress *hid*-induced apoptotic cell death.

Related to Figure 2

(Aa) Eye from a wild type animal. (Ab) Eye from a control animal that expresses *hid* specifically in the eye disc (*GMR-hid*). (Ac) Eye from an animal that expresses *hid* and *p35*. (Ad) Eye from

an animal that expresses hid and *CG11665^{IR}*. (Ae) Eye from an animal that expresses hid and *CG5805^{IR}*. (Af) Eye from an animal that expresses hid and *CG13384^{IR}*. (Ag) Eye from an animal that expresses hid and *CG8177^{IR}*. (Ah) Eye from an animal that expresses hid and *CG10413^{IR}*. (Ba) Eye from a wild type animal. (Bb) Eye from a control animal that expresses Eiger specifically in the eye disc (*GMR-egr*). (Bc) Eye from an animal that expresses Eiger and *p35*. (Bd) Eye from an animal that expresses Eiger and *Bsk^{IR}*. All animals were 3-5 days old.

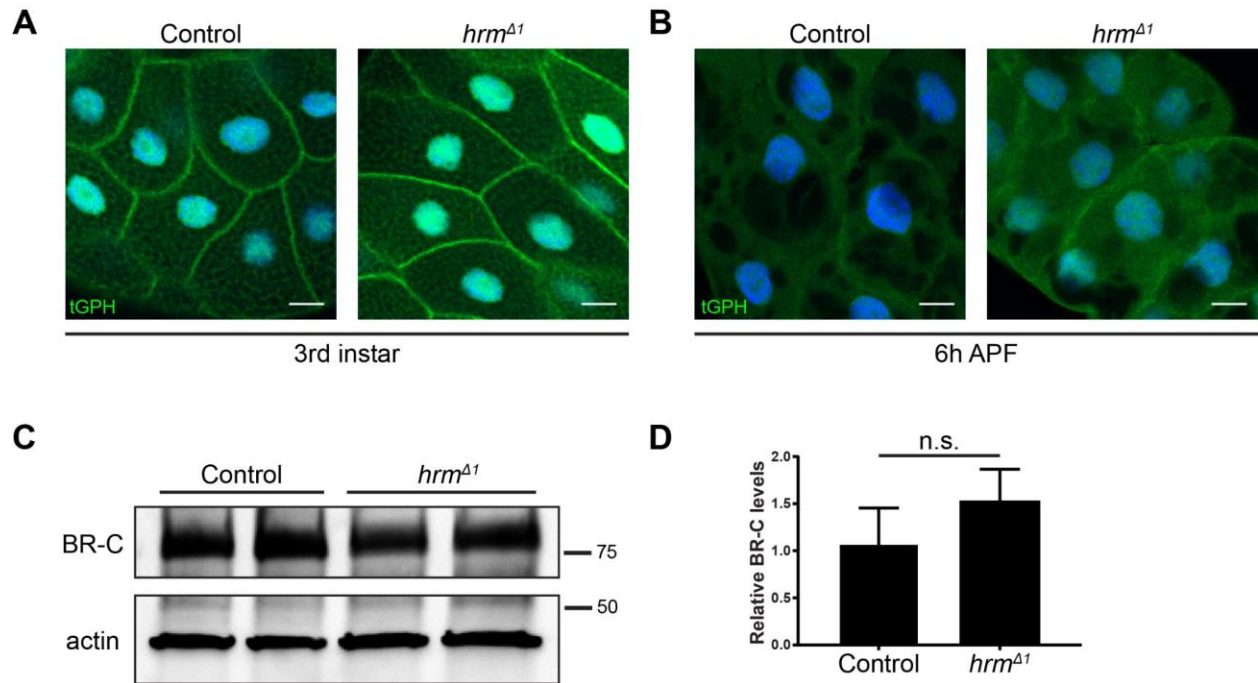


Figure S3. Loss of *hermes* neither influences cell growth nor hormone signaling. Related to Figure 3

(A) Salivary gland tGPH analyses in feeding 3rd instar larvae from control (left) and *hrm^{Δ1}* animals (right). Scale bars represent 20 μ m. (B) Salivary gland tGPH analyses in 13.5h after puparium formation pupae from control (left) and *hrm^{Δ1}* animals (right). Scale bars represent 20 μ m. (C) Western blot analyses of BR-C and actin 13.5 h after puparium formation in salivary gland extracts from control (*w; hrm^{Δ1}/+; +*), n=4, and *hrm* mutant animals (*w; hrm^{Δ1}/Df(2R)BSC696; +*), n=4. (D) Quantification of data from (C). All samples are normalized to actin and plotted relative to control sample. Data are represented as mean \pm SEM. Statistical significance was determined using a Student's t test.

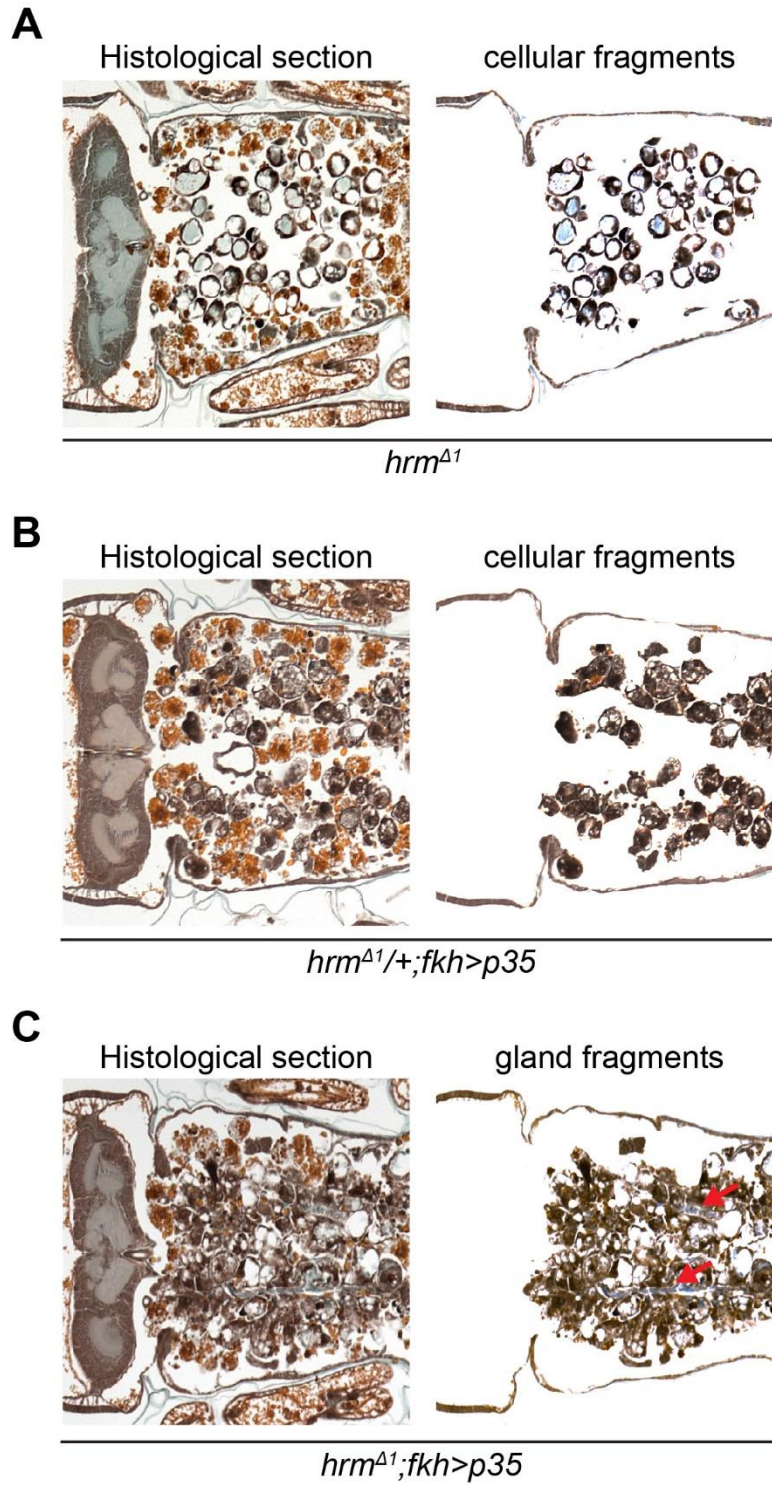


Figure S4. Description of different salivary gland degradation phenotypes. Related to Figure 4

(A) and (B) Histological sections (left) 24h after puparium formation of animals with partially degraded salivary glands resulting in a cellular fragment phenotype [(A) *w; hrm^{Δ1}/Df(2R)BSC696; fkh-GAL4/+*, (B) *w; hrm^{Δ1}/+; fkh-GAL4/UAS-p35*]. The surrounding tissues have been removed to emphasize the remaining salivary gland tissue (right). Note the diffuse nature of the salivary gland material. (C) Histological section (left) 24h after puparium formation of an animal with partially degraded salivary glands resulting in a gland fragment phenotype (*w; hrm^{Δ1}/Df(2R)BSC696; fkh-GAL4/UAS-p35*). The surrounding tissues have been removed to emphasize the remaining salivary gland tissue (right). Note that the remaining salivary gland tissue retains its basic glandular structure (arrows) and is less diffuse than in (A) or (B).

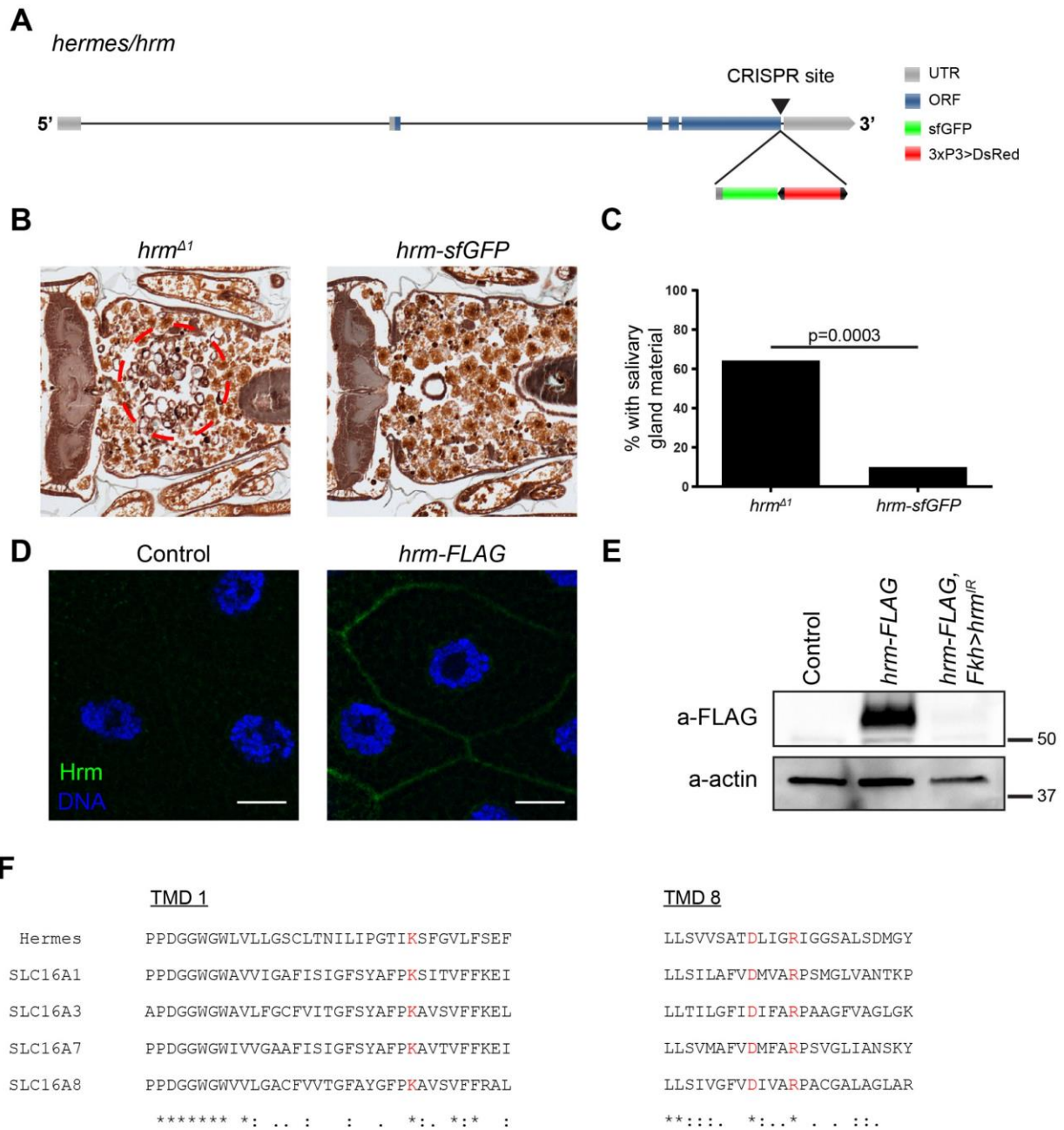


Figure S5. *hermes* encodes a plasma membrane monocarboxylate transporter. Related to Figure 6

(A) Schematic representation of *hermes*. The arrow indicate the CRISPR targeted site where the sfGFP sequence was inserted. (B) Samples from control *hrm* mutants animals (*w*;

hrm^{Δ1}/*Df(2R)BSC696*; +), n=20 (left) and *hrm-sfGFP* animals (*w*; *hrm-sfGFP/Df(2R)BSC696*; +), n=20 (right), analyzed by histology for the presence of salivary gland material (red dotted circle) 24h after puparium formation.. (C) Quantification of data from (B). Statistical significance was determined using a Chi-square test. (D) Salivary glands dissected from control 3rd instar larvae (*w*; +; +) (left), *hrm-FLAG* larvae (*w*; *hrm-FLAG*; +), (right) stained with FLAG antibody (green) and Hoechst (blue). Scale bars represent 20μm. (E) Western blot analyses of FLAG and actin in salivary gland extracts from control (*w*; +; +), *hrm-FLAG* (*w*; *hrm-FLAG*; +) and *hrm-FLAG* with salivary gland specific *hrm* downregulation (*w*; *hrm-FLAG*; *Fkh-GAL4/hrm^{IR}*) 3rd instar larvae. (F) Sequence alignment of transmembrane domains (TMDs) 1 and 8 from *hrm* and SLC16 category I family members. Residues conserved in SLC16 category I members are indicated in red.

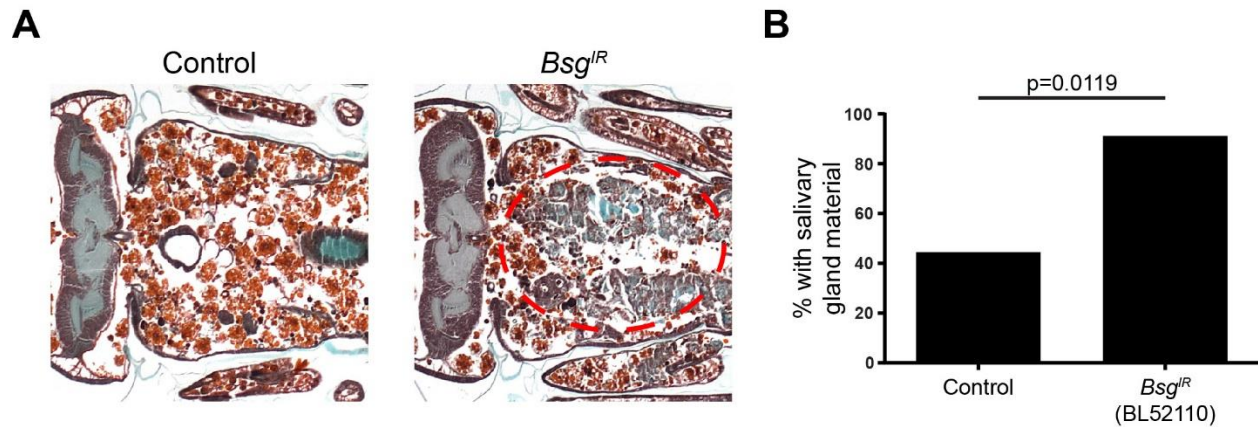


Figure S6. Down-regulation of *Bsg* results in persistence of salivary gland material.

Related to Figure 6

(A) Samples from control animals ($w/+; UAS-Bsg^{IR}/+; +$), $n = 13$ (left), and those with salivary gland-specific knockdown of *Bsg* ($fkh-GAL4/w; UAS-Bsg^{IR}/+; +$), $n = 11$ (right), analyzed with histology for the presence of salivary gland material (red dotted circle) 24h after puparium formation. (B) Quantification of data from (A). Statistical significance was determined using a Chi-square test.

FlyBase Number	Common Name	Human ortholog (DIOPT v6)	RNAi line	% with fragments	p
FBgn0033028	CG11665	SLC16A11	v7314	100.00%	0.0001
			BL52902	85.00%	0.0001
FBgn0039223	CG5805	SLC25A44	v35592	95.83%	0.0001
			BL57571	62.50%	0.0004
FBgn0032036	CG13384	SLC36A4	BL41703	95.00%	0.0001
			v106698	75.00%	0.4011
FBgn0036043	CG8177	SLC4A2	v109594	91.30%	0.0001
			BL51827	16.67%	
FBgn0031676	senju	SLC35A5	v13399	95.83%	0.0001
			v110668	66.67%	0.0001
FBgn0034611	MFS16	SLC37A2	v6591	87.50%	0.0001
			v108635	54.17%	0.0005
FBgn0036732	Oatp74D	SLCO1A2	v37295	95.83%	0.0001
FBgn0032123	Oatp30B	SLCO5A1	v110237	62.50%	0.0001
			v22983	50.00%	0.0001
FBgn0032689	CG10413	SLC12A9	v103780	66.67%	0.002
			BL58307	25.00%	
FBgn0037203	slif	SLC7A1	v110425	54.17%	0.0001
			v45590	8.33%	
FBgn0039714	Zip99C	SLC39A13	BL50635	62.50%	0.0316
			v1362	25.00%	
FBgn0036770	Prestin	SLC26A5	BL50706	62.50%	0.002
			v5341	8.33%	
FBgn0036816	Indy	SLC13A2	v9981	25.00%	
			v9982	50.00%	0.0899
FBgn0035173	CG13907	SCL16A14	v107339	45.83%	
FBgn0011603	ine	SLC6A13	BL51919	41.67%	
			v8880	33.33%	
FBgn0029896	CG3168	SLC22A20	BL29301	41.67%	
			v48010	0.00%	
FBgn0036116	CG7888	SLC36A3	v37263	33.33%	
			v37264	33.33%	
FBgn0034494	CG10444	SLC5A6	v4722	16.67%	

			v107008	33.33%	
FBgn0037140	CG7442	SLC22A5	BL35817	8.33%	
			v106555	33.33%	
FBgn0033234	CG8791	SLC17A4	BL34728	33.33%	
			v7945	0.00%	
FBgn0028563	sut1	SLC2A5	v104983	16.67%	
			v9950	16.67%	
FBgn0035432	ZnT63C	SLC30A1	v105145	16.67%	
FBgn0031250	Ent1	SLC29A1	BL51055	8.33%	
			v109885	8.33%	
FBgn0019952	Orct	SLC22A4	BL60125	0.00%	
			v6782	0.00%	
FBgn0031038	Tyler	SLC25A40	N/A		

TableS1. SLC genes that are upregulated before salivary gland degradation. Related to Figure 1